

## Modelling of Li-ion batteries using equivalent circuit diagrams

**Abstract.** This paper presents the fundamentals of a method how to determine the state of charge (SOC) of lithium-ion batteries on the basis of two different equivalent circuit diagrams and an extended Kalman filter (EKF). It describes how to identify the parameters of these circuits by characteristic measurements. The comparison between measurement and computation results shows a good accordance. In the first step the dependency of these parameters on the temperature and on the battery age is neglected.

**Streszczenie.** W artykule przedstawiono podstawy metody pozwalającej określić stan naładowania (SOC) akumulatorów litowo-jonowych na podstawie dwóch różnych schematów zastępczych i rozszerzonego filtru Kalmana (EKF). Opisano, jak zidentyfikować parametry akumulatorów na podstawie pomiarów ich charakterystyk. Porównanie wyników pomiarów z wynikami symulacji wykazuje zgodność. W pierwszym etapie pominięto zależność parametrów akumulatorów od temperatury i od czasu użytkowania. (Modelowanie akumulatorów litowo-jonowych z wykorzystaniem schematów zastępczych)

**Keywords:** Li-ion battery, equivalent circuit diagrams, battery modelling, parameters identification.

**Słowa kluczowe:** akumulator Li-Ion, schematy zastępcze, modelowanie baterii, identyfikacja parametrów.

### Introduction

If a defined full charge of a battery takes place regularly it is possible to determine the state of charge (SOC) by the so-called Ampere-counting method. This method is basing on the charge that is transferred into the battery respectively taken out of the battery. In case where a defined full charge of the battery cannot happen regularly the error in the SOC estimation can become unacceptable high and a better method has to be found. The SOC is a function of the open circuit voltage (OCV) of a lithium-ion battery,  $SOC=f(V_{OC})$ , but this method involves the problem of its dynamics as Figures 3 (c) and (d) demonstrate. The electrochemical processes which take place in a cell result in the fact that the OCV cannot be measured at the battery terminals. The dynamics needs to be modeled mathematically in a way that the OCV respectively SOC can be calculated by measuring only the battery voltage and current at the terminals of the battery. For this purpose an equivalent circuit diagram for the battery cell has to be used, and the parameters need to be identified by characteristic measurements.

In this paper at first the internal resistance model (IR) is presented, then the one time constant model (OTC), and finally the two time constants model (TTC). Further, comparisons between the model-based simulation data and the measured data are carried out to evaluate the validity of the demonstrated models, which provide a foundation for the model based SOC estimation [4].

### Equivalent Circuit models

**IR Model.** the IR model as shown in Figure 1 (a), and described by Equation 1 implements an ideal voltage source  $V_{OC}$  that represents the open-circuit voltage (OCV) of the battery, and an ohmic resistance in order to describe the internal resistance. Both, resistance and open-circuit voltage  $V_{OC}$  are functions of SOC, state of health (SOH) and temperature.  $i_{Batt}$  is the battery output current with a positive value when discharging, and a negative value when charging,  $v_{Batt}$  is the battery terminal voltage [1].

$$(1) \quad v_{Batt} = V_{OC} - R_0 i_{Batt}$$

As the IR model does not represent the transient behavior of lithium-ion cells, it is not suitable for the accurate estimation of SOC during any dynamical operation (non-constant load).

**OTC Model.** The OTC model adds a parallel RC network in series to the internal resistance  $R_0$  of the IR model, in order to approximate the dynamic behaviour of

the lithium-ion battery. As shown in Figure 1 (b), it mainly consists of three parts including the voltage source  $V_{OC}$ , the ohmic resistance  $R_0$ , and  $R_{OTC}, C_{OTC}$  to describe the battery transient response during charging or discharging.  $v_{OTC}$  is the voltage across  $C_{OTC}$ ;  $i_{OTC}$  is the current that flows in  $C_{OTC}$ . The electric behaviour of the OTC model can be expressed by Equations 2 and 3 in continuous time [1]:

$$(2) \quad \dot{v}_{OTC} = \frac{-I}{R_{OTC} * C_{OTC}} v_{OTC} + \frac{I}{C_{OTC}} i_{Batt},$$

$$(3) \quad v_{Batt} = V_{OC} - v_{OTC} - R_0 i_{Batt}.$$

The description in discrete time is shown by Equations 4 and 5.

$$(4) \quad v_{OTC,k+1} = v_{OTC,k} e^{\frac{-T_s}{\tau_{OTC}}} + R_{OTC} \left( I - e^{\frac{-T_s}{\tau_{OTC}}} \right) i_{Batt,k}$$

$$(5) \quad v_{Batt,k} = V_{OC}(SOC_k) - v_{OTC,k} - R_0 i_{Batt,k}$$

where:  $T_s$  – sampling period,  $\tau_{OTC}$  – OTC time constant.

**TTC Model.** Basing on the observation of the battery output voltage when the battery output current is zero (no-load) it has been found out that the battery shows a big difference between the short time and the long time transient behavior. That means the dynamic characteristics cannot be represented very accurately by the OTC model.

To improve the flexibility of the OTC model an extra RC network is added in series to the OTC circuit to get the TTC circuit model. As shown in Figure 1 (c), the TTC circuit is composed of four parts: voltage source  $V_{OC}$ , ohmic resistance  $R_0$ ,  $R_{TTC1}$  and  $C_{TTC1}$  to describe the short term characteristics,  $R_{TTC2}$  and  $C_{TTC2}$  to describe the long term characteristics.  $v_{TTC1}$  and  $v_{TTC2}$  are the voltages across  $C_{TTC1}$  and  $C_{TTC2}$  respectively.  $i_{TTC1}$  and  $i_{TTC2}$  are the outflow currents of  $C_{TTC1}$  and  $C_{TTC2}$  respectively [1].

The electrical behavior of the TTC circuit can be expressed by Equations 6, 7 and 8 in continuous time:

$$(6) \quad \dot{v}_{TTC1} = \frac{-I}{C_{TTC1} R_{TTC1}} v_{TTC1} + \frac{I}{C_{TTC1}} i_{Batt},$$

$$(7) \quad \dot{v}_{TTC2} = \frac{-I}{C_{TTC2} R_{TTC2}} v_{TTC2} + \frac{I}{C_{TTC2}} i_{Batt},$$

$$(8) \quad v_{Batt} = V_{OC} - v_{TTC1} - v_{TTC2} - R_0 i_{Batt}.$$

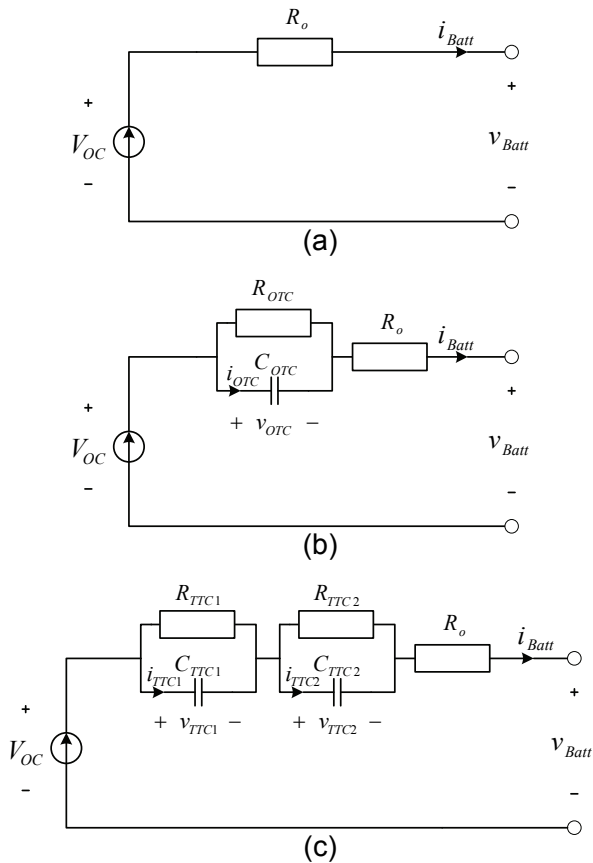


Fig.1. Battery equivalent circuit diagrams. (a) internal resistance model (IR), (b) one time constant model (OTC), (c) two time constants model (TTC).

The description in discrete time is given by Equations 9, 10 and 11:

$$(9) \quad v_{TTC1,k+1} = \frac{-T_s}{\tau_{TTC1}} e^{\frac{-T_s}{\tau_{TTC1}}} + R_{TTC1} \left( 1 - e^{\frac{-T_s}{\tau_{TTC1}}} \right) i_{Batt,k},$$

$$(10) \quad v_{TTC2,k+1} = \frac{-T_s}{\tau_{TTC2}} e^{\frac{-T_s}{\tau_{TTC2}}} + R_{TTC2} \left( 1 - e^{\frac{-T_s}{\tau_{TTC2}}} \right) i_{Batt,k},$$

$$(11) \quad v_{Batt,k} = V_{OC}(SOC_k) - v_{TTC1,k} - v_{TTC2,k} - R_0 i_{Batt}.$$

### Estimation of Model Parameters

In this section the procedure of estimating the model parameters basing on battery measurements is demonstrated. In a first approach temperature and aging effects are neglected. The experimental parameter identification of the battery has been performed at the constant temperature of 25°C with relatively new and unused cells. The temperature and aging effects will be taken into account in a continuation of this work.

**Charging and Discharging Process.** Figure 2, shows characteristic curves of the battery output voltage and current when charging and discharging. In the following the different subintervals of the curves are described:

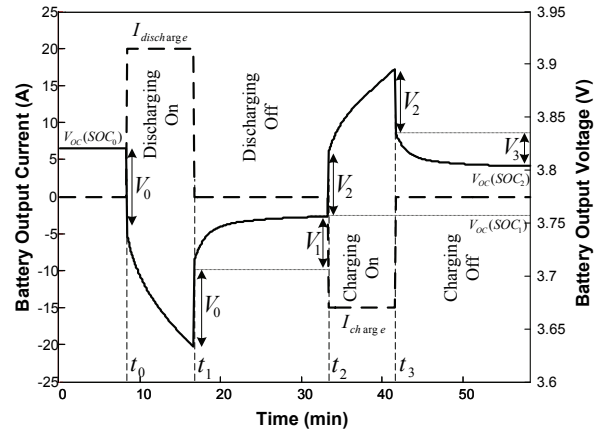


Fig.

2. Characteristic waveforms for battery output voltage and current during charging and discharging of lithium-ion cells.

- Subinterval  $S_0(t < t_0)$ : In this subinterval the battery output current can be assumed to zero over a sufficient time, though the output voltage can reach the open circuit voltage value  $V_{OC}(SOC_0)$ , and while the output current is zero the SOC value is constant.
- Subinterval  $S_1(t_0 \leq t \leq t_1)$ : In this subinterval the battery is discharged with a constant current  $I_{discharge} > 0$ , first a steep decrease of the battery output voltage can be seen due to the internal resistance  $R_0$ , and then it continues to decrease exponentially controlled by the OCV (as the SOC is decreasing).
- Subinterval  $S_2(t_1 \leq t \leq t_2)$ : In this subinterval the battery output current  $i_{Batt} = 0$ , so the battery output voltage at first will have a steep increase due to  $R_0$ , and then it shows an exponential increase until it reaches  $V_{OC}(SOC_1)$ .
- Subinterval  $S_3(t_2 \leq t \leq t_3)$ : In this subinterval the battery is charged with a constant current  $I_{charge} < 0$ , at first a steep increase of the battery output voltage can be seen due to internal resistance  $R_0$ , and then it continues to increase exponentially controlled by the OCV (as the SOC is increasing).
- Subinterval  $S_4(t \geq t_3)$ : In this time subinterval the battery output current  $i_{Batt} = 0$ , so the battery output voltage at first will have a steep decrease due to  $R_0$ , and then it has an exponential decrease until it reaches  $V_{OC}(SOC_2)$ .

**Ohmic Resistance.** The voltage drop across  $R_0$  at the first time instant when charging ( $V_2$ ) respectively discharging ( $V_0$ ) can be taken to calculate  $R_0$  [2], according to Equation 12:

$$(12) \quad R_0 = \begin{cases} \frac{V_0}{I_{discharge}} & \text{for discharging} \\ \frac{-V_2}{I_{charge}} & \text{for charging} \end{cases}.$$

**Estimation of OTC Model Parameters.** In this step battery output voltage measurements during the subintervals  $S_2$  and  $S_4$  are used, as in these subintervals OCV is constant, and the battery output voltage is just driven by the dynamic characteristics of the battery. The output voltage  $v_{Batt}$  during  $S_2$  and  $S_4$  can be calculated according to the OTC model by setting  $i_{Batt}$  to zero in Equations 2 and 3, then solving the differential equation as shown in Equation 13:

$$(13) \quad \begin{cases} S_2 : v_{Batt}(t) = V_{OC}(SOC_1) - v_{OTC}(t_1) e^{\frac{-t}{\tau_{OTC}}} \\ S_4 : v_{Batt}(t) = V_{OC}(SOC_2) - v_{OTC}(t_3) e^{\frac{-t}{\tau_{OTC}}} \end{cases},$$

where:

$$(14) \quad \tau_{OTC} = R_{OTC}C_{OTC}.$$

The identification of OTC model parameters necessitates the estimation of the values  $V_{OC}(SOC_1)$ ,  $V_{OC}(SOC_2)$ ,  $v_{OTC}(t_1)$ ,  $v_{OTC}(t_3)$  and  $\tau_{OTC}$  in Equations 13 and 14. In order to estimate these parameters a nonlinear least squares algorithm is applied (nonlinear data fitting) to search for the values which lead to the best fit between the given measurements and the nonlinear function (in this case an exponential function  $f(t)=A+Be^{-at}$  is used).

The output of the nonlinear least squares algorithm is a vector of the coefficients  $A$ ,  $B$  and  $\alpha$ . These coefficients will be used to calculate the OTC model parameters through Equations 15 to 19:

$$(15) \quad \begin{cases} S_2 : V_{OC}(SOC_1) = A, v_{OTC}(t_1) = B \\ S_4 : V_{OC}(SOC_2) = A, v_{OTC}(t_2) = B' \end{cases}$$

$$(16) \quad \tau_{OTC} = \frac{1}{\alpha},$$

$$(17) \quad \begin{cases} T_{discharge} = t_1 - t_0 \\ T_{charge} = t_3 - t_2 \end{cases},$$

$$(18) \quad \begin{cases} S_2 : R_{OTC} = \frac{v_{OTC}(t_1)}{\left(1 - e^{-\frac{-T_{discharge}}{\tau_{OTC}}}\right) I_{discharge}} \\ S_4 : R_{OTC} = \frac{v_{OTC}(t_3)}{\left(1 - e^{-\frac{-T_{charge}}{\tau_{OTC}}}\right) I_{charge}} \end{cases},$$

$$(19) \quad C_{OTC} = \frac{\tau_{OTC}}{R_{OTC}}.$$

**Estimation of TTC Model Parameters.** TTC model parameters can be estimated the same way as for the OTC model, by taking into consideration the two RC networks instead of one in the OTC model. The TTC model output voltage can be expressed during the subintervals  $S_2$  and  $S_4$  by Equations 20 and 21:

$$(20) \quad \begin{cases} S_2 : v_{Batt} = V_{OC}(SOC_1) - v_{TTC1}(t_1)e^{-\frac{-t}{\tau_{TTC1}}} - v_{TTC2}(t_1)e^{-\frac{-t}{\tau_{TTC2}}} \\ S_4 : v_{Batt} = V_{OC}(SOC_2) - v_{TTC1}(t_3)e^{-\frac{-t}{\tau_{TTC1}}} - v_{TTC2}(t_3)e^{-\frac{-t}{\tau_{TTC2}}} \end{cases},$$

Table 1. SLPB120216216 Cell Data

Typical Capacity		53 Ah
Nominal Voltage		3.7 V
Charge Condition	Max. Current	53A
	Voltage	4.2 ± 0.03 V
Discharge Condition	Continuous Current	159 A
	Peak Current	260 A
	Cut-off Voltage	3.0 V

where:

$$(21) \quad \begin{cases} \tau_{TTC1} = R_{TTC1}C_{TTC1} \\ \tau_{TTC2} = R_{TTC2}C_{TTC2} \end{cases}.$$

The identification of the TTC model requires to estimate the values  $V_{OC}(SOC_1)$ ,  $V_{OC}(SOC_2)$ ,  $v_{TTC1}(t_1)$ ,  $v_{TTC1}(t_3)$ ,  $v_{TTC2}(t_1)$ ,  $v_{TTC2}(t_3)$ ,  $\tau_{TTC1}$  and  $\tau_{TTC2}$  in Equations (20) and (21). In this case an exponential function with two time constants  $f(t)=A+Be^{-at}+Ce^{-\beta t}$  is used.

The output of the nonlinear least squares algorithm is a vector of the coefficients  $A$ ,  $B$ ,  $C$ ,  $\alpha$ , and  $\beta$ . These coefficients will be used to calculate all TTC model parameters through Equations 22 to 27:

$$(22) \quad \begin{cases} S_2 : V_{OC}(SOC_1) = A \\ S_4 : V_{OC}(SOC_2) = A' \end{cases}$$

$$(23) \quad \begin{cases} S_2 : v_{TTC1}(t_1) = B, v_{TTC2}(t_1) = C \\ S_4 : v_{TTC1}(t_3) = B, v_{TTC2}(t_3) = C' \end{cases}$$

$$(24) \quad \begin{cases} \tau_{TTC1} = \frac{1}{\alpha} \\ \tau_{TTC2} = \frac{1}{\beta} \end{cases}$$

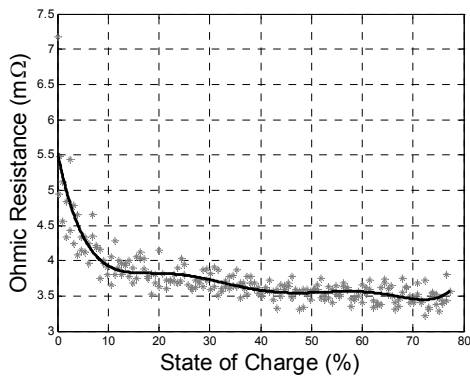
$$(25) \quad \begin{cases} S_2 : R_{TTC1} = \frac{v_{TTC1}(t_1)}{\left(1 - e^{-\frac{-T_{discharge}}{\tau_{TTC1}}}\right) I_{discharge}} \\ S_4 : R_{TTC1} = \frac{v_{TTC1}(t_3)}{\left(1 - e^{-\frac{-T_{charge}}{\tau_{TTC1}}}\right) I_{charge}} \end{cases},$$

$$(26) \quad \begin{cases} S_2 : R_{TTC2} = \frac{v_{TTC2}(t_1)}{\left(1 - e^{-\frac{-T_{discharge}}{\tau_{TTC2}}}\right) I_{discharge}} \\ S_4 : R_{TTC2} = \frac{v_{TTC2}(t_3)}{\left(1 - e^{-\frac{-T_{charge}}{\tau_{TTC2}}}\right) I_{charge}} \end{cases},$$

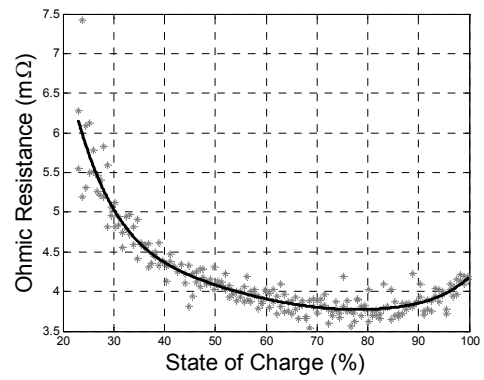
$$(27) \quad \begin{cases} C_{TTC1} = \frac{\tau_{TTC1}}{R_{TTC1}} \\ C_{TTC2} = \frac{\tau_{TTC2}}{R_{TTC2}} \end{cases}.$$

### Experimental and Computational Results

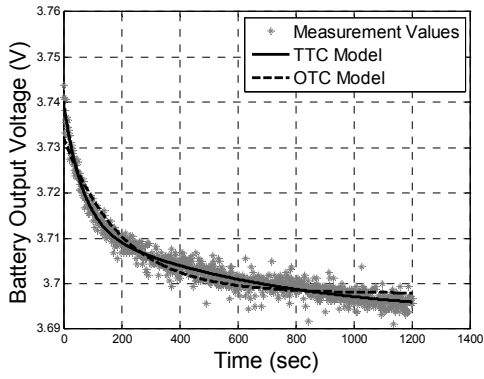
For the experimental tests and modeling lithium polymer battery cells from the manufacturer Kokam have been used. Some important cell data are depicted in Table 1. To identify the model parameters, a battery test bench was set up. In this test bench a current signal with rectangular shape has to be applied to the battery with short and long interrupts. At the same time the battery output voltage has to be measured. The ohmic resistance  $R_0$  of the battery can be calculated during short interrupts of the current signal, while OTC and TTC model parameters need to be estimated during long interrupts.



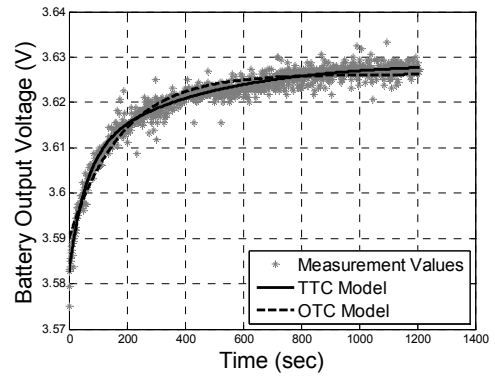
(a)



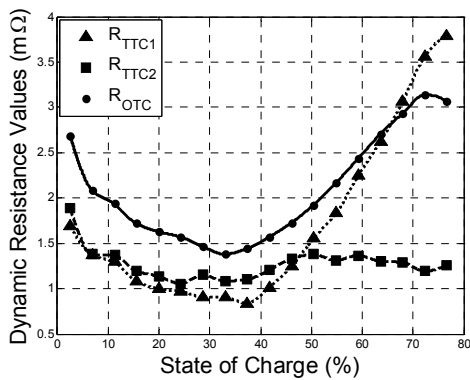
(b)



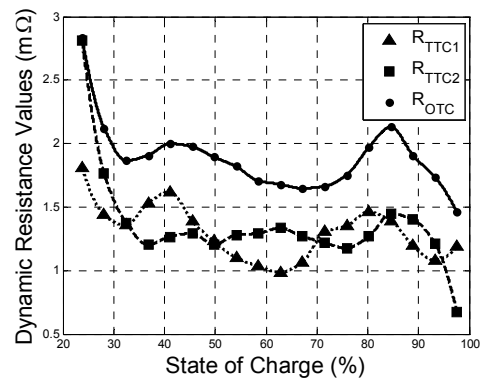
(c)



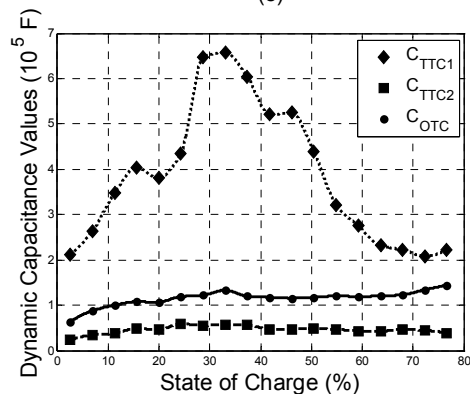
(d)



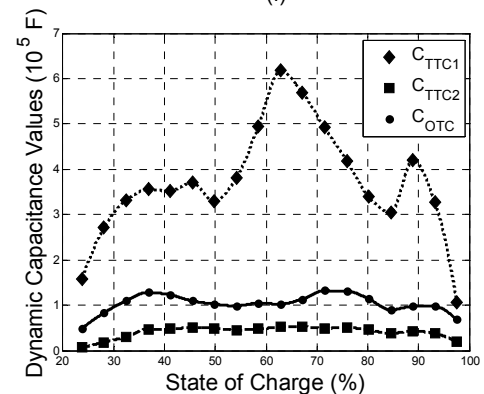
(e)



(f)



(g)



(h)

Fig. 3. (a), (b): ohmic resistance  $R_o$  as a function of SOC during charging and discharging processes respectively; (c), (d): output voltage measurement and computational results during charging and discharging processes respectively; (e), (f): dynamic resistance values as a function of SOC during charging and discharging processes respectively; (g), (h): dynamic capacitance values as a function of SOC during charging and discharging processes respectively.

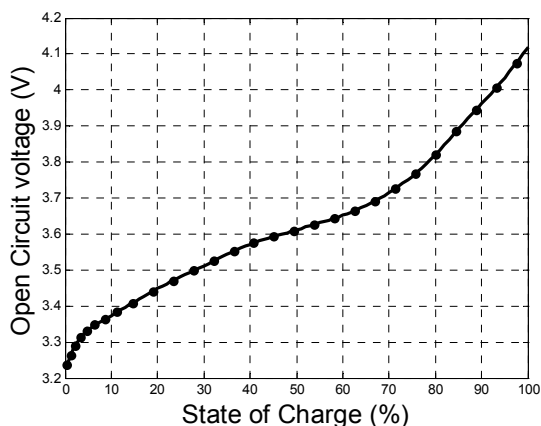


Fig. 4. Battery open circuit voltage as a function of SOC.

### Experimental and Computational Results

For the experimental tests and modeling lithium polymer battery cells from the manufacturer Kokam have been used. Some important cell data are depicted in Table 1. To identify the model parameters, a battery test bench was set up. In this test bench a current signal with rectangular shape has to be applied to the battery with short and long interrupts. At the same time the battery output voltage has to be measured. The ohmic resistance  $R_0$  of the battery can be calculated during short interrupts of the current signal, while OTC and TTC model parameters need to be estimated during long interrupts.

**Ohmic Resistance Results:** Ohmic resistance  $R_0$  results are shown in Figures 3 (a) and (b) for charging and discharging processes respectively. It can be seen that  $R_0$  increases at low SOC values in both, charging and discharging processes.

**Values of the RC-Network Elements:** Figures 3 (c) and (d), depict the battery output voltage measurement with the OTC and TTC model values for one long interrupt during charging and discharging processes respectively at 25°C. This processes are repeated over all long interrupts. From these two figures it can be seen that the TTC model has a better fit to the measurements than the OTC model, therefore the TTC model gives a better representation of the battery dynamics compared to the OTC model.

Dynamic resistance values are shown in Figures 3 (e) and (f) in both, charging and discharging processes respectively. These two figures demonstrate that there is not such a big deviation in the dynamic resistance values as it is the case with the dynamic capacitances. Dynamic capacitance values are depicted in Figures 3 (g) and (h) during both, charging and discharging processes respectively.

In these figures it can be seen that  $C_{TTC1}$  has a value being about 10 times greater than  $C_{TTC2}$ , that leads to a greater time constant  $\tau_{TTC1}$  which is responsible for the long

term effects in the battery. Figure 4 shows the battery open circuit voltage in dependence of SOC.

### Conclusion

This paper presents three different equivalent circuit diagrams for lithium-ion batteries. The IR model is a very simple model, but it does not represent at all the dynamics of the battery and therefore it is not suitable for an accurate SOC determination during any dynamical operation. The OTC model describes the dynamic characteristics of the battery approximately (Figures 3 (c) and (d)). By adding a second RC network the dynamics of the lithium-ion battery can be approximated very accurately (Figures 3 (c) and (d)), thus a good estimation of SOC can be expected.

This paper demonstrates how to identify the parameters of the equivalent circuit diagrams of lithium-ion cells from characteristic measurements. The next step of this research consists of the application of an Extended Kalman Filter to obtain the optimum estimation of SOC. A comparison of the results with the Ampere-counting method will be shown.

### Acknowledgment

The authors wish to thank the Federal Ministry of Economics of Germany for the financial support by the research projects eE-Tour (Electric Mobility) and IRENE (Integration of Renewable Energy and Electric Mobility). Further many thanks to Prof. Dr. R. Schmidt, President of the University of Applied Sciences Kempten, and Prof. Dr.-Ing. A. Rupp, Vice President for R&D, for their continuous support of the Institute for Applied Battery Research.

The publication of this paper was supported by the European Social Fund (project "Doctoral School of Energy and Geotechnology II").

### REFERENCES

- [1] Hongwen He, Rui Xiong, and Jinxin Fan, "Evaluation of Lithium-Ion Battery Equivalent Circuit Models for State of Charge Estimation by an Experimental Approach," *J. Energies*, vol. 4, pp 582-598, ISSN 1996-1073, March 2011.
- [2] Hans-Georg Schweiger et al, "Comparison of Several Methods for Determining the Internal Resistance of Lithium-Ion Cells," *J. Sensors*, vol. 10, pp. 5604-5625, ISSN 1424-8220, June 2010.
- [3] G. Plett, "Extended Kalman Filtering for Battery Management Systems of LiPB-Based HEV Battery Packs. Part 1. Background," *J. Power Sources*, vol. 134, pp. 252-261, 2004.
- [4] Giacomo Marangoni, "Battery Management System for Li-Ion Batteries in Hybrid Electric Vehicles," M. Sc. thesis, Dept. of Information Engineering, University of Padova, Padua, Italy, 2010.

**Authors:** prof. dr.-ing. Helmuth Biechl, University of Applied Sciences Kempten, Bahnhofstraße 61, 87435 Kempten, Germany, E-mail: [biechl@fh-kempten.de](mailto:biechl@fh-kempten.de); dipl.-ing. Ahmad Rahmoun, University of Applied Sciences Kempten, Bahnhofstraße 61, 87435 Kempten, Germany, E-mail: [ahmad.rahmoun@fh-kempten.de](mailto:ahmad.rahmoun@fh-kempten.de).